Atmospheric and Oceanic Science Letters

ISSN: 1674-2834 (Print) 2376-6123 (Online) Journal homepage: https://www.tandfonline.com/loi/taos20

Micro-Pulse Lidar Measurements of Aerosol Vertical Structure over the Loess Plateau

Huang Jian-Ping, Huang Zhong-Wei, Bi Jian-Rong, Zhang Wu & Zhang Lei

To cite this article: Huang Jian-Ping, Huang Zhong-Wei, Bi Jian-Rong, Zhang Wu & Zhang Lei (2008) Micro-Pulse Lidar Measurements of Aerosol Vertical Structure over the Loess Plateau, Atmospheric and Oceanic Science Letters, 1:1, 8-11, DOI: 10.1080/16742834.2008.11446756

To link to this article: https://doi.org/10.1080/16742834.2008.11446756

ATMOSPHERIC AND OCEANIC SCIENCE LETTERS, 2008, VOL. 1, NO. 1, 8–11

Micro-Pulse Lidar Measurements of Aerosol Vertical Structure over the Loess Plateau

HUANG Jian-Ping, HUANG Zhong-Wei, BI Jian-Rong, ZHANG Wu, and ZHANG Lei

College of Atmospheric Sciences, Lanzhou University, Lanzhou 730000, China

Received 14 May 2008; revised 10 June 2008; accepted 16 June 2008; published 16 November 2008

Abstract Knowledge of the vertical distribution of aerosols in the free troposphere is important for estimating their impact on climate. In this study, direct observations of the vertical distribution of aerosols in the free troposphere are made using surface Micro-Pulse Lidar (MPL) measurements. The MPL measurements were made at the Loess Plateau (35.95°N, 104.1°E), which is near the major dust source regions of the Taklimakan and Gobi deserts. The vertical distribution of the MPL backscattering suggested that non-dust aerosols floated from ground level to an altitude of approximately 9 km around the source regions. Early morning hours are characterized by a shallow aerosol layer of a few hundred meters thick. As the day progresses, strong convective eddies transport the aerosols vertically to more than 1500 m.

Keywords: lidar, aerosol, vertical structure, Loess Plateau

Citation: Huang, J. P., Z. W. Huang, J. R. Bi, et al., 2008: Micro-pulse lidar measurements of aerosol vertical structure over the Loess Plateau, *Atmos. and Oceanic Sci. Lett.*, **1**, 8–11.

1 Introduction

The vertical distribution of dust aerosols is a critical problem in estimating the effect of dust on radiative forcing and its associated climate impacts (Claquin et al., 1998; Zhu et al., 2007; Forster et al., 2007). An analysis of observations by Minnis and Cox (1978) and a model study by Carlson and Benjamin (1980) showed that an elevated Saharan dust layer could change the atmospheric heating rate dramatically. Liao and Seinfeld (1998) claimed that clear sky long-wave radiative forcing and cloudy sky top-of-atmosphere (TOA) short-wave (SW) radiative forcing are very sensitive to the altitude of the dust layer. Meloni et al. (2005) found that SW aerosol radiative forcing at the TOA has a strong dependence on aerosol vertical profiles.

Prior to the availability of actively sensed data, the normal method of analyzing aerosols depended on the collection of aerosol samples on filters and chemically analyzing them to obtain the mass concentration of different aerosol species. These are then converted to number distribution and subsequently to optical depths using Mie scattering theory (Satheesh and Ramanathan, 2000). Surface-measured properties are converted to column properties by making assumptions about vertical profiles. In many cases, the surface aerosol properties are entirely different from the column aerosol properties due to the presence of distinct aerosol layers aloft (Ramanathan et al., 2001). Thus, the assumption that different days have the same aerosol vertical profile can result in large errors (as much as by a factor of two) (Satheesh, 2002). Surface LIDAR, however, offer the possibility to accurately determine the vertical structure of dust aerosols and their related physical properties, in order to improve the quantification and reduce the uncertainty of aerosol radiative forcing. Micro-Pulse Lidar (MPL) has been widely used all over the world. For example, MPL observations were used by Niranjan (2007) to characterize the temporal/spatial distributions of high altitude aerosol layers in India, and by Powell et al. (2000) to identify and profile elevated Saharan dust layers during the Aerosol Characterization Experiment-2 (ACE-2). Cloud and aerosol studies also benefit from extended MPL observations (Campbell et al., 2002), both for Atmospheric Radiation Measurement (ARM) and similarly motivated global satellite monitoring programs. Zhou et al. (1998) discussed optical properties of troposphere aerosols determined by home-made L300 lidar measurements. Qiu et al. (2003) analyzed characteristics of the upper troposphere cloud and aerosols in Beijing using their home-made multi-wavelength lidar. However, until now the quantitative discussions of the vertical structure of aerosol related to LIDAR observations have been rather scarce over Northwest China. Our MPL measurements should lead to reliable analysis of aerosol vertical structure, and expand the understanding of the impact of aerosols on climate.

2 Micro-Pulse LIDAR (MPL)

The MPL Network (MPLnet) LIDAR (Welton et al., 2001) was installed in April 2007 at the Lanzhou University Semi-Arid Climate & Environment Observatory of Lanzhou University (SACOL) (Huang et al., 2008), located on the Loess Plateau (35.95°N, 104.1°E) in Northwest China (Fig. 1). It provided real-time backscatter vertical profile images during day and night. The MPL system employs an optical transceiver that acts as both transmitter and receiver (telescope) and consists of a pulsating Nd:YLF laser at 527 nm, an Avalanche Photo Diode (APD) photon counting detector, a signal processing unit, and a data processor. The laser pulse duration was 100 ns, which gives a vertical resolution of 75 m. The range corrected, normalized LIDAR return signal for one transmitted laser pulse is a combination of the backscatter energy

Corresponding author: HUANG Jian-Ping, hjp@lzu.edu.cn

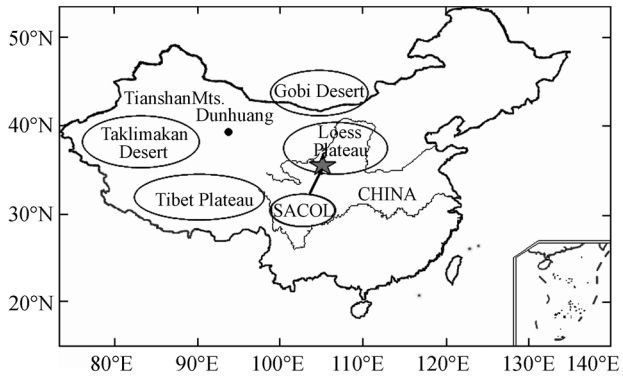

Figure 1 Location of the semi-arid climate & environment of Lanzhou Unversity (SACOL), where the surface Micro-Pusle Lidar is operated at SACOL.

from Rayleigh and aerosol components. The color maps shown here are the backscatter intensity after range, overlap, and Rayleigh correction, and represent the aerosol backscatter intensity only as a function of altitude. An AERONET-Cimel sun photometer for spectral radiative and aerosol optical properties (Holben et al., 1998) has been used to contrast the aerosol column integrated features. Additional information about the MPL and SACOL information is available at http://climate.lzu.edu.cn.

The MPL has been in operation at SACOL 24 hours a day, seven days a week since April 2007. The data set used in this study covers 55 days during spring (April–May) 2007. Cloudy profiles are screened based on a simple cloud-aerosol discrimination method. The backscattered intensities from clouds are generally stronger than those from aerosols, which can be used to separate clouds from aerosols. Thus, cloudy profiles are screened for backscattered intensities greater than 1, and the screened values are filled with linearly fit values. The fit value is interpolated using the data above and below the cloud layer.

3 Retrieval method

Aerosol layer optical depths τ can be calculated in terms of backscatter of MPL, i.e.,

$$\tau = \int_{r_1}^{r_2} \sigma_1(r)\mathrm{d}r \,, \tag{1}$$

where σ_1 is the aerosol extinction coefficient retrieved from the attenuated backscatter intensity according to Fernald (1984):

$$\sigma_1(r) = -\frac{S_1}{S_2}\sigma_2(r) + \frac{\ln[P(r)]\exp\left[2\left(\frac{S_1}{S_2}-1\right)\int_r^{r_c}\sigma_2(r')\mathrm{d}r'\right]}{\frac{\ln[P(r_c)]}{\sigma_1(r_c)+\frac{S_1}{S_2}\sigma_2(r_c)} + \int_r^{r_c}\ln[P(r')]\exp\left[2\left(\frac{S_1}{S_2}-1\right)\int_r^{r_c}\sigma_2(r'')\mathrm{d}r''\right]}, \tag{2}$$

$P(r)$ is the backscatter intensity after all corrections except for the MPL dimensional system calibration constant C (Campbell et al., 2002). r is the range from lidar to the particles; σ_2 is the local atmosphere molecule extinction coefficient, calculated from the atmosphere molecule density vertical structure obtained from the American standard atmosphere model using Mie scattering theory; S_1 is the product of the aerosol extinction-to-backscatter ratio 20–70; and S_2 is the atmosphere molecule extinction-to-backscatter ratio usually equal $8\pi/3$.

4 Preliminary results

Figure 2 shows a typical spring normalized relative back scatter intensity as a function of local time and altitude, collected by surface MPL at SACOL on 18 May 2007.

As shown in Fig. 2, aerosols are mostly confined to a light layer of 2 km thickness during the night and morning. However, strong aerosol backscatter was observed in the afternoon and early evening (1300–1900 LST) between 1 to 3 km, with a thin aerosol layer extending to 10 km. Plume-like structures of enhanced aerosol concentration are clearly visible during this period. These structures suggest that the presence of strong turbulent mixing lifts the aerosols upwards from near-surface levels. According to the meteorological record, 18 May is a typical clear day over the Loess Plateau. The lower altitude aerosol layers are possibly due to locally-generated aerosols.

Figure 3 compares the MPL integrated aerosol optical depths with aerosol column optical depths obtained using CIMEL sun photometer (CE318) observations at 527 nm during daytime. The measurements agree well, as the LIDAR-derived contribution of aerosol extinction, due to the layers, matches that observed from the column aerosol optical depths (AODs) within ±2% for this date.

Figure 4 shows daytime averaged (0900–1900 LST) and seasonal (April and May) averaged vertical profiles of aerosol extinction coefficients retrieved by the MPL measurements at SACOL. Strong aerosol extinction was observed from an altitude of 1 to 3 km. Additional peaks can be found at 9 km, indicating high altitude aerosol layers. The lower altitude peak is possibly due to locally generated aerosols, while the high altitude peak is most likely due to convective lifting of aerosols originating from distant sources transported by horizontal upper air movement. The larger error bar at lower altitude peak suggests the strong variability of local aerosol.

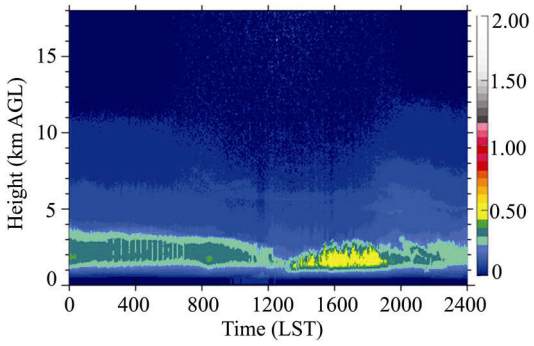

Figure 2 Daily variation of MPL normalized relative backscattering at SACOL for 18 May 2007.

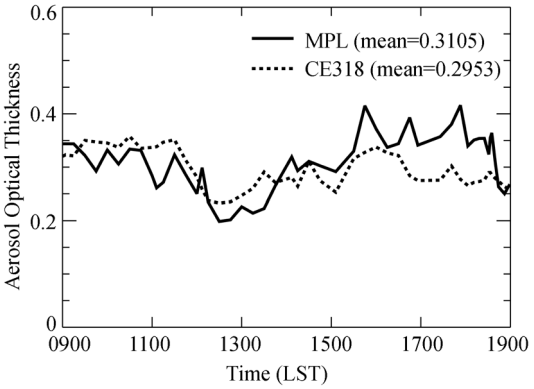

Figure 3 Comparison of MPL derived aerosol optical depth (AOD) with Sun photometer derived AOD for 18 May 2007. The wavelength of AOD is at 527 nm.

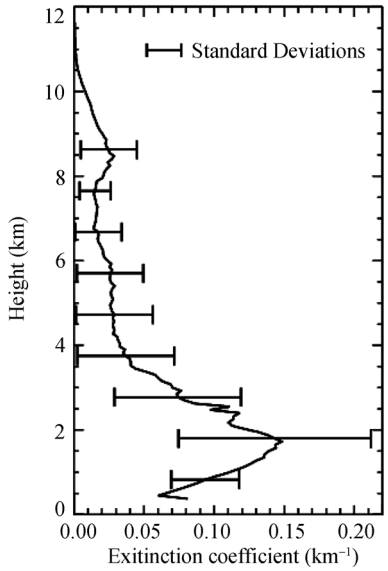

Figure 4 Daytime (0900−1900 LST) and seasonal (April and May) averaged vertical profile of MPL aerosol extinction coefficients. Error bars are standard deviations computed from vertical bins of each profile.

5 Discussion and Conclusions

The preliminary results discussed above are only based on surface MPL measurements taken during a short time period, and do not cover a sufficient time span to definitely conclude that the observed aerosol vertical distributions are predominant for the Loess Plateau region. Long term monitoring and analysis will be necessary to determine typical aerosol vertical distributions and transport mechanisms for the region. Further research should focus on combining MPL measurements with other SACOL surface aerosol instruments and A-Train satellite measurements.

The MPL and other observational facilities of SACOL represent a unique resource for climate research, and should allow the community to focus its effort on the high priority problem of understanding the semi-arid climate. The SACOL's integrated dataset is being used to improving understanding of aerosol-climate interaction, and to test and improve climate model and satellite remote sensing techniques. MPL and other data from SACOL can be accessed online at http://climate.lzu.edu.cn.

Acknowledgments. This research is supported by the National Natural Science Foundation of China under Grant Nos. 40628005 and 40633017.

References

Carlson, T. N., and S. G. Benjamin, 1980: Radiative heating rates for Saharan dust, *J. Atmos. Sci.*, **37**(1), 193–213.

Claquin, T., M. Schulz, Y. J. Balkanski, et al., 1998: Uncertainties in assessing radiative forcing by mineral dust, *Tellus*, **50**(B), 491–505.

Campbell, J. R., D. L. Hlavka, E. J. Welton, et al., 2002: Full-time, eye-safe cloud and aerosol lidar observation at atmospheric radiation measurement program sites: Instruments and Data Processing, *J. Atmos. & Ocean. Tech.*, **19**, 431–442.

Fernald, F. G., 1984: Analysis of atmospheric lidar observations-Some comments, *Appl. Opt.*, **23**, 652–653.

Forster, P., V. Ramaswamy, P. Artaxo, et al., 2007: Changes in atmospheric constituents and in radiative forcing. In: *Climate Change 2007*: *The Physical Science Basis, Working Group I to the Fourth Assessment Report of the Intergovernmental Panel on Climate Change,* United Kingdom and New York: Cambridge University Press, Cambridge, 129–234.

Holben, B. N., T. F. Eck, I. Slutsker, et al., 1998: AERONET—A federated instrument network anddata archive for aerosol characterization, *Remote Sens. Environ.,* **66**, 1–16.

Huang, J., W. Zhang, J. Zuo, et al., 2008: An overview of the semi-arid climate and environment research observatory over Loess Plateau, *Advance in Atmospheric Sciences*, accepted and in press.

Liao, H., and J. H. Seinfeild,1998: Radiative forcing by mineral dust aerosols: Sensitivity to key variables, *J. Geophys. Res*., **103** (D24), 31637–31645.

Meloni, D., A. D. Sarra, T. D. Iotio, et al., 2005: Influence of the vertical profile of Saharan dust on the visible direct radiative forcing, *J. Quant. Spectrosc. Radiat. Transfer*, **93**, 397–413.

Minnis, P., and S. K. Cox, 1978: Magnitude of the radiative effects of the Sahara dust layer, Ft. Collins, Colo.: Colo. State Univ., *Atmos. Sci.* Pap., 111–283.

Niranjan, K., B. L. Madhavan, and V. Sreekanth, 2007: Micro pulse lidar observation of high altitude aerosol layers at Visakhapatnam located on the east coast of India, *Geophys. Res. Lett.*, **34**, L03815, doi:10.1029/2006GL028199.

Powell, D. M., J. A. Reagan, M. A. Rubio, et al., 2000: ACE-2 multiple angle micro-pulse lidar observations from Las Galletas, Tenerife, Canary Islands, *Tellus*, **52**(B), 652–661.

Qiu J., S. Zheng, Q. Huang, et al., 2003: Lidar Measurements of Cloud and Aerosol in the Upper Troposphere in Beijing, *Chinese Journal of Atmospheric Sciences* (in Chinese), **27**, 1–7.

Ramanathan, V., P. J. Crutzen, J. Elieveld, et al., 2001: Indian Ocean experiment: An integrated analysis of the climate forcing and effects of the great Indo-Asian haze, *J. Geophys. Res.*, **106**(D22), 28371–28398.

Satheesh, S. K., 2002: Aerosol radiative forcing over land: Effect of surface and cloud reflection, *Ann. Geophys.*, **20**(12), 2105–2109.

Satheesh, S. K., and V. Ramanathan, 2000: Large difference in tropical aerosol forcing at the top of the atmosphere and Earth's

surface, *Nature*, **405**, 60−63.

Welton, E. J., J. R. Campbell, J. D. Spinhirne, et al., 2001: Global monitoring of clouds and aerosols using a network of micropulse LIDAR systems, *Proc. LIDAR Remote Sensing for Industry and Environmental Monitoring*, **4153**, 151−158.

Zhu, A., V. Ramanathan, F. Li, et al., 2007: Dust plumes over the Pacific, Indian, and Atlantic oceans: Climatology and radiative impact, *J. Geophys. Res*., **112**, D16208, doi:10.1029/2007JD 008427.

Zhou, J., G. Yue, F. Qi, et al., 1998: Optical Properties of Aresols Derived from Lidar Measurements, *Chinese Journal of Quantum Electronics* (in Chinese), **15**, 140−148.